Chapter I

Introduction and Literature Review

1.1 Fuel Cell

The concept of fuel cell was demonstrated in the early nineteenth century by Humphry Davy. William Grove, a chemist and physicist was generally credited with inventing the fuel cell in 1839. He conducted a series of experiments on a gas voltaic battery and proved that electric current could be produced from an electrochemical reaction between hydrogen and oxygen over a platinum catalyst. The term fuel cell was first used in 1889 by Charles Langer and Ludwig Mond who tested fuel cells using coal gas as a fuel.

Fuel cells are electrochemical devices which convert chemical energy in fuels into electrical energy and produce heat from a fuel and oxygen. Unlike conventional engines, fuel cells are clean and more efficient energy devices because these produce only water as a byproduct i.e. friendliness to the environment. Fig. 1.1 shows the operating principle of a fuel cell. It consists of three main parts an anode, a cathode and an electrolyte. Air is supplied to the cathode and fuel is supplied to the anode (in this case H_2) which is oxidized releasing electrons. Electrons pass to the cathode where they reduce the oxygen at the electrode/ electrolyte interface. The electrolyte is the medium through which ions from the cathode reach the anode. Both anode and cathode should be porous in order to be permeable to gas.

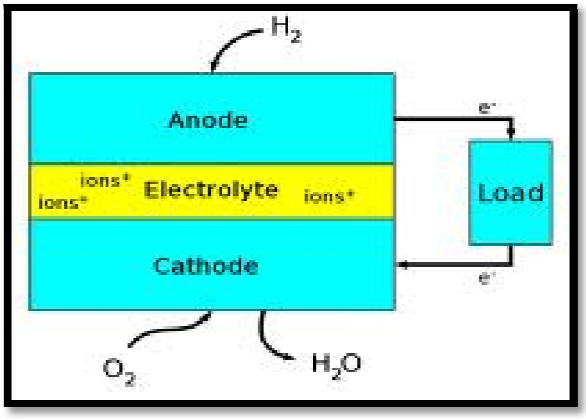

Anode Reaction: $2H_2 + 2O^{-2} \rightarrow 2H_2O + 4e^-$

Cathode Reaction: $O_2 + 4e^- \rightarrow 2O^{-2}$

Overall Cell Reaction: $2H_2 + O_2 \rightarrow 2H_2O$

Fig. 1.1 Working principle of fuel cell [http://www4.nau.edu]

During fuel cell operation, the cell voltage becomes lower than the open circuit voltage due to three major losses:

- Ohmic polarization
- Concentration polarization
- Activation polarization

Fig. 1.2 shows the schematic diagram of polarization curve of a fuel cell. It can be noted from Fig. 1.2 that activation polarization dominates when the current density is low. Ohmic loss is linearly dependent on current density and follows Ohm's law. It can be minimized by reducing the thickness of the electrolyte. Concentration polarization dominates at higher current density.

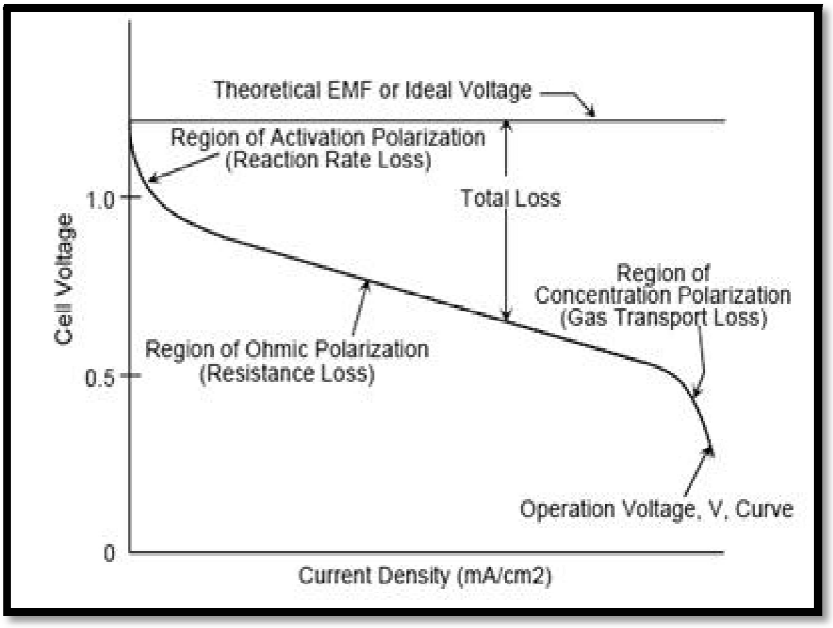

Fig. 1.2 Polarization curve of fuel cell [http//www.altenergymag.com]

1.1.1 Activation polarization

Activation polarization results from the kinetics of electrochemical reactions. Electrochemical reactions have certain barrier which must be overcome in order to proceed. This leads to polarization. Activation polarization is given by Butler-Volmer equation as given below:

$$\eta_{act} = \frac{RT}{\beta zF} \ln\left(\frac{i}{i_0}\right) \tag{1.1}$$

where R, T, β, z, F, i and i_0 are gas constant, operating temperature, electron transfer coefficient, electrons associated with electrochemical reaction, Faraday's constant, operating current and exchange current density respectively. Losses due to activation polarization can be minimized by modifying the morphology of triple phase boundary (TPB). Activation polarization decreases with increasing the TPB length. Larger the TPB length, more will be the reactions which occur. This decreases the polarization.

1.1.2 Ohmic polarization

The ohmic losses results from the electrical resistance of the electrodes and the resistance to the flow of ions in the electrolyte. These losses follow Ohm's law i.e. voltage drop is proportional to the current.

$$\Delta V_{ohm} = iR \tag{1.2}$$

where i is the current density and R is the specific resistance (Ω-cm). Ohmic losses can be minimized by use of highly conducting electrodes and by reducing the thickness of the electrolyte.

1.1.3 Concentration polarization

Losses due to concentration polarization result from change in the concentration of the reactants at the electrodes. During cell operation oxygen is supplied in the form of the air, the change in concentration will cause a change in partial pressure of oxygen. Same thing happens on the anode side. In both the cases reduction in the gas pressure results in a reduction of the voltage drop. If H_2 is fed on the anode side, then the voltage drop caused by change in hydrogen pressure can be given as:

$$\Delta V = \frac{RT}{zF}\, ln\left(\frac{P_2}{P_1}\right) \tag{1.3}$$

Assume restrictive current density, i_l at which the fuel is used at a rate equal to its maximum supply speed. The current density cannot rise above this value, because the fuel gas cannot be supplied at a greater rate. If P_1 is the pressure when the current density is zero, then the current density losses is (i_l – 0). If P_2 is the pressure when the current density is i, then the current density losses are (i_l-i). The relationship between P and current density is given by:

$$P_2 = P_1 \left(1 - \frac{i}{i_1}\right) \quad (1.4)$$

Combining equations 1.3 & 1.4, the change in voltage due to change in hydrogen gas pressure is expressed as:

$$\Delta V = \frac{RT}{zF} ln\left(1 - \frac{i}{i_1}\right) \quad (1.5)$$

This equation represents the voltage change due to the mass transport losses related to the current density.

1.2 Why Fuel Cells

Conversion of chemical energy into electrical energy via processes involves a conventional heating cycle, which is limited by the Carnot's cycle. Heat engines work according to the principle of indirect energy conversion, where heat is primarily produced, then converted into mechanical energy and finally into electrical energy. So in a conventional process, the chemical energy of fossil fuels is converted into electrical energy after several steps comprising a chemical reactor, mechanical engines and electrical generators, where each step causes energy losses. Fuel cells can minimize these losses by converting chemical energy to electrical energy directly and without any Carnot cycle limitations. Apart from the high efficiency of fuel cells, they also exhibit very low emissions, and especially the use of H_2 as a fuel produces only water as by-product [Kordesch et al. (1990)]. Fuel cells produce no vibrations and noise during operation. It helps users avoid the heavy smoke accompanying diesel generators. Compared with solar, wind and other alternative energies, fuel cells require less space and can operate stably 24 hours/365 days regardless the weather and geographic constraints.

1.3 Types of Fuel Cells

There are various types of fuel cells. These are generally classified on the basis of the electrolyte used because the electrolyte determines the operating temperature of a system and in part the kind of fuel that can be employed.

1.3.1 Polymer electrolyte membrane fuel cells (PEMFC)

In PEMFCs design, a proton- conducting polymer (Nafion) membrane (electrolyte) separates the anode and cathode sides. On the anode side, hydrogen diffuses to the anode catalyst where it dissociates into protons and electrons. The protons diffuse through the membrane to the cathode. The electrons are forced to travel in an external circuit (supplying power) because the membrane is electronically insulating. On the cathode catalyst, oxygen molecules react with the electrons (which have traveled through the external circuit) and protons to form water. PEMFC operates in the temperature range 70-110 °C. There is water, air and temperature management problem in using PEMFC. Overall the cell reaction is:

$$H_2 = 2H^+ + 2e^- \quad Anode\ reaction \tag{1.6}$$

$$\frac{1}{2}O_2 + 2H^+ + 2e^- = 2H_2O \quad Cathode\ reaction \tag{1.7}$$

1.3.2 Alkaline fuel cells (AFC)

AFCs have an aqueous solution of sodium hydroxide or potassium hydroxide as the electrolyte. The fuel is almost always hydrogen gas and oxygen is an oxidizer. AFCs generally operate at less than 100 °C and are constructed from metals and certain plastics. Electrodes are made of carbon and a metal such as nickel. Water, as a reaction product, must be removed from the system, usually by evaporation from the electrolyte either through the electrodes or in a separate evaporator. The operating support system presents a significant design problem. The strong, hot alkaline electrolyte attacks most plastics and tends to penetrate structural seams and joints. Overall efficiencies range from 30 to 60%. Overall cell reaction is as follows:

$$H_2 + 2OH^- = 2H_2O + 2e^- \quad Anode\ reaction \tag{1.8}$$

$$\frac{1}{2}O_2 + H_2O + 2e^- = 2OH^- \quad Cathode\ reaction \tag{1.9}$$

1.3.3 Phosphoric acid fuel cells (PAFCs)

Such cells have phosphoric acid as an electrolyte which allows operation up to 200 °C. These can use a hydrogen fuel contaminated with carbon dioxide and an oxidizer, air or oxygen. The electrodes consist of catalyzed carbon and arranged in pairs set back-to-back

to create a series generation circuit. The framing structure for this assembly of cells is made of graphite which markedly raises the cost. The higher temperature and aggressive hot phosphate create structural design problems. Phosphoric acid fuel cells have been proposed and tested on a limited scale for local municipal power stations and for remote-site generators. The reactions at anode and cathode sides are given below:

$$H_2 = 2H^+ + 2e^- \quad Anode\ reaction \tag{1.10}$$

$$\frac{1}{2}O_2 + 2H^+ + 2e^- = 2H_2O \quad Cathode\ reaction \tag{1.11}$$

1.3.4 Molten carbonate fuel cell (MCFC)

The fuel consists of a mixture of hydrogen and carbon monoxide generated from water and a fossil fuel. The electrolyte is molten potassium lithium carbonate, which requires an operating temperature of about 650 °C. Warming up to operational temperatures may take several hours, making these cells unsuitable for vehicles. In most cases, the electrodes are metals based. Operation at high temperatures creates a design problem for long-lived system parts and joints, especially if the cells must be heated and cooled frequently. Overall efficiencies range from 45 to 50%. Fuel cell reactions are:

$$H_2 + CO_3^{2-} = H_2O + CO_2 + 2e^- \quad Anode\ reaction \tag{1.12}$$

$$\frac{1}{2}O_2 + CO_2 + 2e^- = CO_3^{2-} \quad Cathode\ reaction \tag{1.13}$$

1.3.5 Solid oxide fuel cells (SOFCs)

Solid oxide fuel cells use a solid electrolyte, most commonly yttria-stabilized zirconia (YSZ). SOFCs are made entirely from solid materials. These are not limited to the flat plane configuration of other types of the fuel cells. SOFCs are often designed as rolled tubes. They require high operating temperatures (800 to 1000 °C) and can be run on a variety of fuels including natural gas. Overall cell efficiency is 60% and when combined with gas turbine system, efficiency goes up to 70%. The reactions taking place at anode and cathode sides are given as:

$$H_2 + O^{2-} = H_2O + 2e^- \quad Anode\ reaction \tag{1.14}$$

$$\frac{1}{2}O_2 + 2e^- = O^{2-} \quad Cathode\ reaction \tag{1.15}$$

1.4 Solid Oxide Fuel Cells

Solid oxide fuel cells are well known and increasing interest in their development has been since the 1960s [Stimming et al. (2002)]. The characteristics features of

SOFCs are oxygen ion conducting solid electrolyte and high operating temperature (650-1000 °C) [Stimming et al. (2002)]. At high temperatures electrode reactions are very fast which allows using non-noble metal electrodes. High operating temperature results in large amount of heat. This makes the SOFCs suited for combined heat and power production.

A solid oxide fuel cell is an energy conversion device that produces electricity by electrochemically combining a fuel and an oxidant across an oxide ion conducting solid electrolyte. The dense electrolyte is sandwiched between two porous and permeable electrodes, the anode (fuel electrode) and cathode (air electrode). In SOFCs stack, single cells are connected in series via a component called interconnect. Owing to the utilization of solid electrolyte and high operating temperature, it offers many advantages over conventional power generating systems in terms of efficiency, reliability, modularity, fuel flexibility and environmental friendliness.

In addition, SOFCs offer the possibility of co-generation with gas turbine power systems to enable full exploitation of both electricity and heat, thereby enhancing the efficiency up to 70%. The electrolyte represents the media through which ions migrate from one electrode to the other leading to a voltage difference between anode and cathode and consequently an electric current flow through an external load. For this reason, the electrolyte must meet the following requirements:

- **(i)** High ionic conductivity
- **(ii)** High electronic resistivity (nearly zero electronic conductivity)
- **(iii)** Thermal expansion compatible with those of the other cell components
- **(iv)** Chemical stability in contact with the two electrodes
- **(v)** Resistance to thermal cycling
- **(vi)** Low fabrication cost

1.5 Working Principle of SOFCs

The working principle of a SOFC is shown in Fig. 1.3. The electrolyte is sandwich between an anode and a cathode. On the cathode side, oxygen reacts with incoming electrons from the external load to become oxygen ions which migrate

through the electrolyte. On the anode side fuel is oxidized by incoming oxygen ions to liberate the electrons which flow through the external electrical circuit. The charge flow in the external circuit is balanced by ionic current flow within the electrolyte. The potential difference across the electrodes drives the electrons through the external circuit. More specifically, oxygen is disassociated and converted into oxygen ions at cathode/electrolyte interface, whereas the electrochemical oxidation of fuel takes place at anode/electrolyte interface. The output voltage under load condition when the current passes through the cell is given by:

$$V = E^0 - IR - \eta_c - \eta_a \qquad (1.16)$$

where E^0 is the Nernst potential of the reactants (Nernst potential is the ideal open

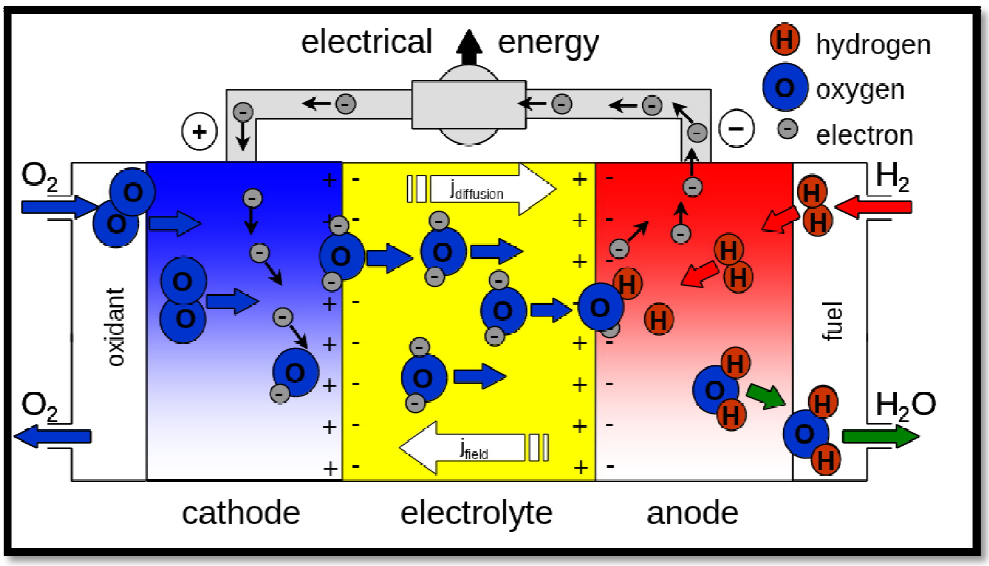

Fig. 1.3 Working Principle of SOFC (http://www.osakagas.co.jp/fuel cell/sofc/img)

circuit potential of the cell), R is the Thevenin equivalent resistance, η_c and η_a define the difference between actual cell voltage and Nernst potential. At the time of operation SOFC can be used either as an oxygen ion conducting electrolyte or a proton conducting electrolyte. The difference in ion activity between the two electrodes results in a driving force for motion of the ions through electrolyte. Thermodynamic efficiency of the cell is given by [Faro et al. (2009)]:

$$\varepsilon = \varepsilon_t \times \varepsilon_v \times \varepsilon_l \quad (1.17)$$

where, ε_t depends on the inherent properties of the fuel. ε_v is related to cell operating voltage and forever less than the theoretical maximum and ε_l is the current efficiency.

1.6. Designs of SOFC

Over the years so many designs of SOFC have been devised starting from pressed thimbles and discs in the 1930s. Recent development has been focused on planer and tubular design SOFCs.

1.6.1 Planer design SOFC

Planer SOFCs have flat plates like cell components which are connected in electrical series [Minh (1993)]. Fig. 1.4 shows the design of planer SOFC.

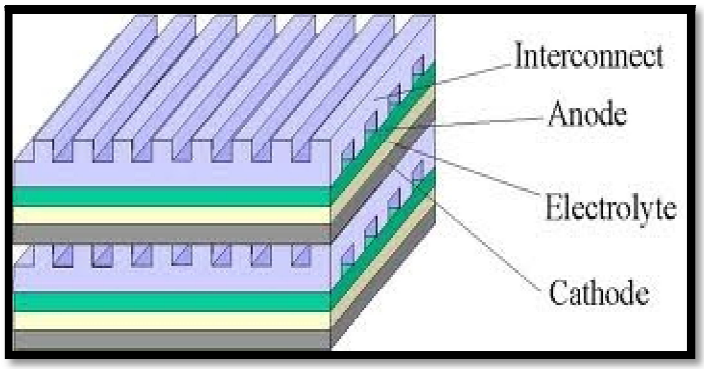

Fig. 1.4 Planer SOFC (http://www.osakagas.co.jp/fuel cell/sofc/img)

The interconnect is ribbed on both the sides, forms gas flow channels and serves as a bipolar gas separator contacting the anode and the cathode of adjoining cells. The cells are fabricated by low-cost conventional ceramic processing techniques such as tape casting, slurry sintering, screen printing, or by plasma spraying [Singhal (2002)]. Recent research has been focused on electrolyte supported, cathode supported and anode supported planer SOFCs. Electrolyte supported cells use yttria stabilized zirconia (YSZ) as an electrolyte of thickness 50-150 µm [Singhal (2002)]. Due to high ohmic resistance, this cell can be used at higher temperature~1000 °C. In electrode supported cells, thickness of the electrolyte is very less of the order of 5-20 µm. This reduces the ohmic resistance and makes

them well suited for low temperature applications~800 ºC. Ni/YSZ cermet anode is used as supported electrode due to its superior thermal and electrical conductivity. Using Ni/YSZ cermat a power density of 1.8 Watt/cm^2 at 800 °C was observed by Kim et al. (1999).

1.6.2 Tubular SOFC

Tubular cell design of SOFC was illustrated by the Siemens Westinghouse shown in Fig. 1.5. Cell components are deposited in the form of thin layers on a doped lanthanum manganite cathode tube [Singhal (2000)].

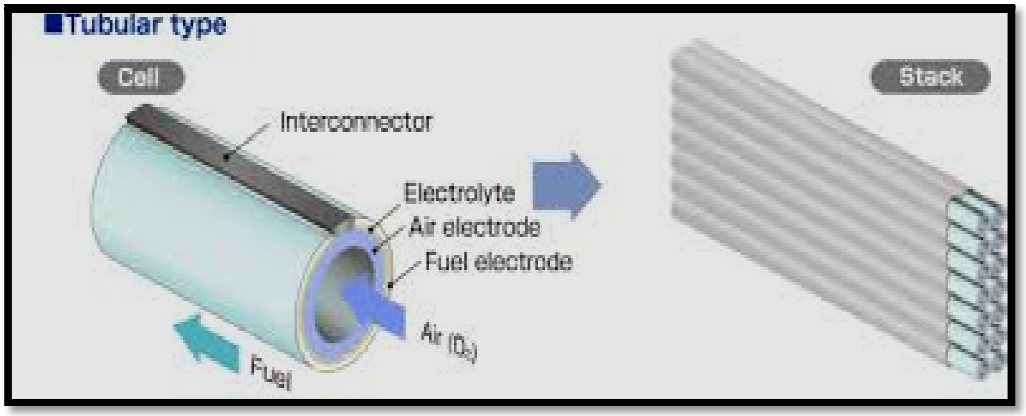

Fig. 1.5 Tubular SOFC (http://www.osakagas.co.jp/fuel cell/sofc/img)

The cathode tube is fabricated by extrusion and sintered YSZ electrolyte is deposited in the form of ~40 μm thick dense layer by electrochemical vapor deposition [Pal et al. (2002)] and the Ni/YSZ anode is deposited either by nickel slurry application followed by electrochemical vapor deposition of YSZ or by sintering of a Ni/YSZ slurry. Doped lanthanum chromite interconnection strip along the length of the cell is deposited by plasma spraying. Such tubular cells have a power density of ~0.25–0.30 W/cm^2 at 1000 °C. Due to low power densities, tubular SOFCs are suitable only for stationary power generation.

1.7 Components of SOFC

1.7.1 Electrolyte

Electrolyte is the main part of the SOFCs through which oxygen ions migrate from cathode to anode without any significant loss. The electrolyte must therefore have following properties:

- High oxygen ion conductivity.
- Zero electronic conductivity.
- Chemically stable in a large oxygen partial pressure gradient from reducing to oxidizing conditions.
- Highly dense to avoid the leakage of gases.
- Thermal expansion well matched with the electrodes.
- Uses low cost materials.
- Thickness of the electrolyte should be very less to reduce the ohmic losses.

Oxygen ions migrate through the electrolyte via oxygen vacancies in the oxygen sub lattice. Among a large number of oxide ion conductors, yttria stabilized zirconia (YSZ) or scandia stabilized zirconia (ScYZ) are the most common electrolytes. YSZ shows conductivity of ~0.1 S/cm at 1000 ºC. To reduce the operating temperature and the cost of the electrolyte, research is going on doped and co-doped ceria electrolytes.

1.7.2 Anode

During the cell operation fuel is fed at the anode side where it will be oxidized in the presence of oxygen ions from the electrolyte. Anode material should have following characteristics:

- It should be a mixed conductor having predominately electronic conductivity to permit the passage of electrons.
- Chemically compatible with other components of the cell.
- Thermal expansion coefficient well matched with the adjoining components.
- Good catalytic activity towards oxidation of fuels.

- Anode should have continuous channels made of pores to allow rapid transport of fuel and reactant gases.
- It should have high carburization and sulfidation resistance.
- Most importantly, anode should be fuel flexible, ease to fabricate and of low cost.

Currently, the most common anode material for SOFC is the porous Ni/YSZ cermat. Because, it is chemically stable in reducing atmosphere at high temperature and its thermal expansion coefficient is closed to that of YSZ [Zhu et al. (2003)]. In the Ni-YSZ cermat, YSZ forms the matrix that prevents Ni from agglomeration which maintains the porous and highly dispersed microstructure [Hacker et al. (2003)]. Ni/YSZ cermat show good performance only for hydrogen but it creates problems with pure or reformed hydrocarbon fuels. Ni has high activity for coke formation which deteriorates the electro catalytic activity and microstructure. Another disadvantage of Ni/YSZ is the re-oxidation of Ni, which involves phase and dimensional changes. To remove these drawbacks, alternatives to Ni/YSZ have been developed for e.g. gadolinium doped ceria, Ti and Y-doped zirconia and lanthanum chromite. Addition of Ni catalyst into the porous ceria a performance of 0.06 Ωcm^2 at 1000 °C in hydrogen atmosphere has been observed [Hacker et al. (2003)]. Ceria based composite anodes Cu/YSZ/ceria [Kim et al. (2001)] and Ni/ceria are being developed for direct application of hydrocarbon fuels [Murray et al. (1999)].

Lanthanum chromite itself is not qualified as anode material due to the poor mechanical response and lattice expansion in reducing atmosphere. However, its desired thermal and chemical stability is highly attractive, and consequently many efforts have been directed towards the exploration of this type of anode. A substitution of La with Sr and Cr with Ti leads to SrTiO3-based materials with n-type conductivity rather than p-type as well as reduced size changes in reducing atmospheres [Zhu et al. (2003)].

1.7.3 Cathode

At the cathode, oxygen is supplied where it reduced to oxide ion which migrates through the electrolyte towards the anode. The cathode environment is highly oxidizing which excludes the use of metals as electrode materials. Cathode materials should have following properties:

- Porous and permeable.
- High electronic conductivity
- Chemically compatible with the other cell's components.
- Highly stable in oxidizing atmosphere.
- High catalytic activity to the dissociation of oxygen.
- High ionic conductivity.
- Thermal expansion coefficient well matched to the adjoining components.
- Ease of fabrication, low cost for wide range of application.

At present, electronically conducting oxide ceramics based on perovskite lanthanum magnenite ($LaMnO_3$) are being used as cathode material. In which La is partially replaced by Sr (strontium doped lanthanum magnenite, LSM), (La, Sr) MnO_3. The electronic conductivity of LSM is around 200 S/cm for Sr concentration of 15% [Hacker et al. (2003)]. Multilayer electrodes are advantageous to optimize the current collection at the cathode. Other electrodes such as $La(Sr)CoO_3$ are better suited as current collectors because of their high electronic conductivity. An improvement in the electro-catalytic activity of LSM has been found by addition of the noble metal catalysts [Hacker et al. (2003)]. The cost for cathode materials can be reduced by using mixture of lanthanides.

1.7.4 Interconnects

Interconnects are used for designing a SOFC stack to connect the multiple cells. It should have high electronic conductivity and should be stable both in highly reducing and oxidizing conditions at the anode and cathode respectively. It should be dimensionally stable in a gradient of partial pressure of oxygen. The thermal expansion coefficient of the interconnect material should be well matching with

the electrodes and the electrolyte. Low permeability for the oxygen and hydrogen to minimize direct combination of the oxidant and the fuel during the cell operation is also a requirement for interconnects. To fulfill these requirements, a p-type doped lanthanum chromite ($LaCrO_3$) is used as an interconnect material. Its conductivity can be enhanced by doping of alkaline earth ions such as Ca, Sr and Mg on the La site or Cr [Singhal (2000)].

1.7.5 Sealing

During design of SOFCs stack sealing plays a very important role. In planer design of SOFCs, sealing is an integral part but there is no requirement of sealing in tubular design SOFCs. Glasses and glass ceramic composites are commonly used as sealing materials.

1.8 Solid Oxide Electrolytes

Solid oxide electrolyte is the major part of the solid oxide fuel cells. It should be highly conducting at the operating temperature of SOFCs. The oxides with open structure have high oxide ion conductivity. Many electrolytes such as; zirconia based, lanthanum gallate based, bismuth oxide based and doped or co-doped ceria have been developed.

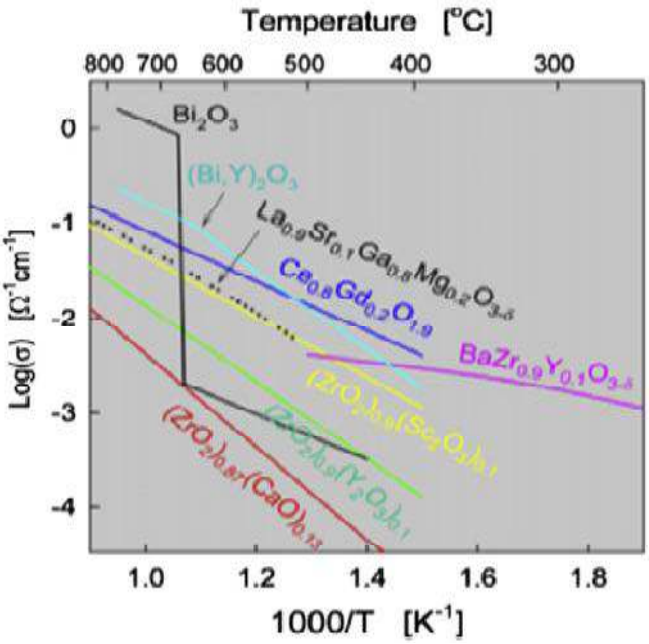

Fig. 1.6 Log σ vs. 1000/T plot of some oxide ion electrolytes [Inba et al. (1996)]

A schematic plot for conductivity of oxide electrolytes is shown in Fig. 1.6. Their advantages and disadvantages are discussed one by one as below.

1.9 High Temperature Electrolytes

1.9.1 Zirconia based electrolytes

Zirconia-based solid electrolytes are regarded as an effective solid electrolyte for SOFC. ZrO_2 has monoclinic structure at room temperature and undergoes a phase transition to tetragonal structure above 1170 ºC. Zirconia has cubic fluorite structure above 2370 ºC. Cubic fluorite structure of zirconia can be stabilized by doping of aliovalent cations. The most commonly dopants are CaO, MgO, Y_2O_3, and Sc_2O_3 [Strickler et al. (1964); Dixon et al. (1963); Guo et al. (2001); Yeh et al. (2005); Yamamoto et al. (1995); Johansen et al. (1964); Hohnke (1980); Lee et al. (2001); Prokhorov et al. (2005); Djurado et al. (2003)]. The maximum ionic conductivity in ZrO_2-based systems is observed when the concentration of accepter type dopants is close to the minimum to completely stabilize the cubic fluorite structure [Etsell et al. (1970); Kharton et al. (1999); Yamamoto et al. (1998); Badwal (1992)]. At present SOFC currently being developed employ yttria stabilized zirconia, (YSZ). YSZ shows adequate level of oxide ion conductivity and desired stability in both oxidizing and reducing atmosphere. Scandia stabilized zirconia (ScSZ) also show desirable conductivity in the range 0.15-0.20 S/cm at 1000 ºC. YSZ fulfills all the requirement high ionic conductivity but problems occur because of its reactivity with pervoskite oxide cathodes containing lanthanum at higher temperature. It reacts with lanthanum forms $La_2Zr_2O_7$ resistive layer [Jacobson (2010)]. High operating temperature of YSZ possesses large number of engineering and material problems.

1.10 Intermediate Temperature Electrolytes

Many efforts have been made to reduce the operating temperature of SOFCs (500-700 ºC) using different type of electrolytes as discussed below. Intermediate temperature solid oxide fuel cells (IT-SOFCs) removes all the problems associated with high working temperature.

1.10.1 Bi_2O_3- based electrolytes

Among oxide ion conducting materials, Bi_2O_3 based solid electrolytes are particularly interesting due to their high ionic conductivity [Bouwmeester et al. (1996); Sammes et al. (1999); Goodenough et al. (1990); Kharton et al. (2001); Shuk et al. (1996)]. Bi_2O_3 shows significant polymorphism with two stable phases, α and δ. High temperature δ-phase shows high conductivity. The stabilization of the δ- Bi_2O_3 phase down to temperatures 973-1073 K can be achieved by replacement of bismuth with rare-earth dopants such as Y, Dy or Er and their combinations with higher valence cations, such as W or Nb [Perfilyev et al. (1988); Sammes et al. (1999) Yaremchenko et al. (1998); Kharton et al. (2001); Shuk et al. (1996); Takahashi et al. (1975); Jian et al. (2002)]. The main drawback of Bi_2O_3 based solid electrolytes is the less stability in reducing atmospheres. There are several ways to overcome these problems, for example by covering with a thin layer resistant to reduction, e.g. of ZrO_2 [Wasiucionek et al. (2006)]. Some problems remain including the ability of δ-Bi_2O_3 to maintain high ionic conductivity at typical working temperatures (~500 ^oC) for long periods of time. Some efforts have been made using an optimal level of doping which provides both high conductivity and long term stability [Jung et al. (2010)].

1.10.2. $LaGaO_3$-based electrolytes

Doped $LaGaO_3$ also has potential as a solid electrolyte in SOFCs. Doped lanthanum gallate possesses higher ionic conductivity than that of stabilized zirconia in the temperature range 770-1100 K [Yasuda et al. (2000); Kim et al. (2001); Stevenson et al. (1998); Ishihara et al. (1994); Feng et al. (1994); Huang et al. (1996); Stevenson et al. (1997); Drenna et al. (1997); Baker et al. (1997); Kharton et al. (1997); Ishihara et al. (1997); Khan et al. (1998); Huang et al. (1998); Ishihara et al. (1998); Trofimenko et al. (1999); Kharton et al. (2000); Slater et al. (1998); Huang et al. (1997)]. High oxide ion conductivity in $LaGaO_3$ can be achieved by substituting alkaline earth ions at La site and/or incorporating divalent metal cations, such as Mg^{2+}, into gallium sublattice in order to increase concentration of oxygen vacancies. High ion conductivity of (Sr, Mg)-doped $LaGaO_3$, of general formula $La_{1-x}Sr_xGa_{1-y}Mg_yO_{3-\delta}$ (LSGM), was first reported in

1994 by Ishihara (1994) and Feng et al. (1994). The existence of two different size cation sites in the pervoskite structure expands the range of possible dopants. For example in addition to strontium and magnesium, barium or gadolinium [Stevenson et al. (1997); Bradley et al. (2003)] can also be doped on lanthanum site. Doping of barium, rather than strontium alters the octahedral tilt angle which reduces activation energy. At high temperatures conductivity of $La_{0.9}Ba_{0.1}Ga_{0.8}Mg_{0.2}O_{2.85}$ is lower than that of $La_{0.9}Sr_{0.1}Ga_{0.8}Mg_{0.2}O_{2.85}$, but the reverse is the case at low temperature [Stevenson et al. (1997); Bradley et al. (2003)]. Other lanthanum based perovskites, including $LaSrO_3$, $LaInO_3$ and $LaYO_3$-based materials are oxygen ion conductors [Chen et al. (2003)].

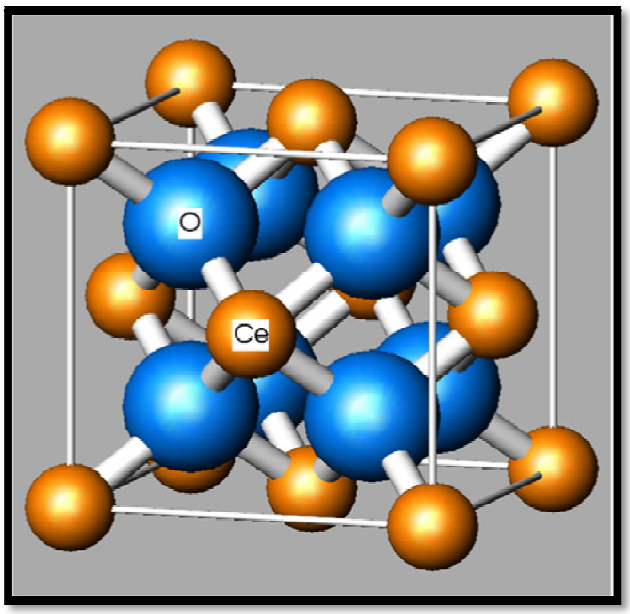

Fig. 1.7 Crystal structure of ceria [http://www.wikipidia.com]

LSGM electrolyte is less employed because of several issues, such as difficulty in obtaining single phase materials, volatility of gallium at high temperatures and its high reactivity with Ni, the latter resulting in formation of the ionically insulating $LaNiO_3$ phase [Huang et al. (1998); Matraszek et al. (2004); Huang et al. (1997)].

1.10.3 Doped and co-doped ceria

Ceria has fluorite structure as shown in Fig. 1.7 and is a common electrolyte for the SOFCs. It has good compatibility with the electrodes [Steele (2000); Zha et al.

(2003); Kuharuangrong (2007)]. Ceria has high ionic conductivity particularly at low temperature as compared to zirconia due to its large ionic radius of 0.97 Á (with 8 fold co-ordinations). The main compensating defect in ceria is the oxygen vacancies.

Samarium (Sm) and gadolinium (Gd) doped ceria were found to be best ionic conductors for IT-SOFCs. $Ce_{0.90}Gd_{0.1}O_{1.95}$ (CGO10) has ionic conductivity of 0.01 S/cm at 500 ºC. In polycrystalline ceramic electrolytes, grain boundary is an extra contribution to the total resistance that is dependent on impurities that segregate to the boundaries. In addition to Gd and Sm other rare earth cations such as lanthanum (La) [Suda et al. (2006); Sha et al. (2007); Shimonosono et al. (2005)] and neodymium [Lai et al. (2005); Yashiro et al. (2004); Sakai et al. (2004)] can also be used as dopants in ceria. The additive effect of alkaline earth oxides such as CaO, SrO, MgO, and BaO as dopants in ceria was studied by Arai et.al. [Brook et al. (1982); Yahiro et al. (1988)]. The addition of CaO and SrO enhances electrical conductivity of ceria and reduces the activation energy. The addition of BaO and MgO, however does not increase the electrical conductivity very much as compared to CaO and SrO due to large size mismatch of Mg^{2+} (0.89 Á), Ba^{2+} (1.42 Á) and the Ce^{4+} (0.97 Á).

Kim proposed the concept of a critical ionic radius for the dopant. This is an ideal dopant cation radius that would give the same lattice constant as that of the undoped ceria [Kim (1989)]. The critical ionic radius for a trivalent and divalent dopant in ceria is 1.038 Á and 1.11 Á respectively [Inaba et al. (1996)]. However, although Gd- or Sm-doped ceria have higher ionic conductivity than Y-doped ceria, the best match for either the ionic radius of Ce^{4+} (0.97 Å) or the critical ionic radius in ceria is Y^{3+} (1.019 Å) rather than Gd^{3+} (1.053 Å) or Sm^{3+} (1.079 Å). Kilner et al. and Catlow [Kilner et al. (1982); Catlow (1984)] proposed that a smaller ionic size mismatch between the host and a dopant leads to enhancement in conductivity.

Enhancing conductivity of CeO_2 and its stability in reducing atmosphere, a co-doping approach was proposed by Herle et al. [Herle et al. (1999)]. They found that co-doping of ceria with two or more cations (alkaline earth and rare earth cations) increases the conductivity more than that of best singly doped ceria in air.

Recently, research has also been made to produce cost effective ceria based solid electrolytes with desired ionic conductivity for IT-SOFCs. Many co-doped ceria electrolytes have been investigated such as; $Ce_{0.85}Gd_{0.1}Mg_{0.05}O_{1.9}$ [Wang et al. (2004)], $Ce_{0.80}Gd_{0.2-x}Sm_xO_{1.9}$ [Kim et al. (2000)] $Ce_{1-x-y}Gd_xPr_yO_{2-z}$ [Lubke et al. (1999)], $Ce_{0.8}Sm_{0.2-x}Y_xO_{1.9}$ [Sha et al. (2006)] etc.

Mori et al. (1999) defined an effective index, E_i to explain the trend in oxide ion conductivity of co-doped ceria electrolytes. They suggested that when co-doped CeO_2 based systems reach the ideal fluorite structure they exhibit maximum ionic conductivity when effective index is close to 1. Effective index, E_i can be defined as:

$$E_i = \frac{avg.r_c}{eff.r_o} \times \frac{r_d}{r_h} \tag{1.18}$$

where $avg.r_c$ is the average ionic radius of the cations, $eff.r_o$ is the effective ionic radius of oxygen ion, r_d is the average ionic radius of the dopants and r_h is the radius of host cation.

Yammamura et al. (2000) reported that ordering of oxygen vacancies is suppressed due to co-doping. This increases the configurational entropy of the system followed by a decrease in the activation energy. This increases the total conductivity. Configurational entropy, S, of a system with constant oxygen vacancies, $Ce_{1-x-y}M'_xM_yO_{2-\delta}$ is given as:

$$S = R[(1-x-y)\ln(1-x-y) + xlnx + ylny] \tag{1.19}$$

where 'R' is the gas constant (8.314 J/mol K). Co-doped ceria systems have high configurational entropy as compared to singly doped ceria.

1.11 Enhancement in Conductivity of Grain Boundaries in Co-Doped Ceria

Grain boundaries in CeO_2 and ZrO_2 based electrolytes are highly resistive in nature. Total ionic conductivity can be increased by reducing the grain boundaries resistance. Alkaline earth cations such as CaO, SrO and MgO were found to be good grain boundaries scavenger [Cho et al. (2009); Cho et al. (2008); Park et al. (2009); Cho et al. (2007)]. Kim et al. (2007) studied the scavenging effect of SrO.

They found that Sr^{2+} reacts with SiO_2 and forms some silicate phases. These phases gather at triple point junction of the grain boundaries leaving clean grain to grain contact area. This reduces the grain boundaries resistance and hence the overall resistance of the electrolytes. Cioatera et al. (2009) also studied the effect of strontium addition on the conductivity of europium-doped ceria. They found a significant decrease of grain boundaries resistance on substituting europium and strontium in the CeO_2. Some other systems were also studied such as; $Ce_{0.80-x}Gd_{0.20}Sr_xO_{2-\delta}$ [Ramesh et al. 2009] and $Ce_{0.80}Y_{0.20-x}Sr_xO_{2-\delta}$ [Zheng et al. (2009)].

Gerhardt et al. (1986) studied the scavenging effect in the yttrium doped ceria. On the basis of scanning transmission electron microscopy (STEM) combined with energy dispersive X-ray microanalysis (EDXM) and electron energy loss spectroscopy (EELS), they found that in yttrium doped ceria an amorphous silica resistive thick layer forms surrounding the grains. This layer blocks the charge carriers leading to increase in the resistivity of the grain boundaries and hence the total resistivity. Gerhardt et al. studied the EDXM spectrum of CeO_2:6.mol% Gd_2O_3 sample and found that the spectrum of a grain and that of a grain boundary (as shown in Fig. 1.8) are not different except for the presence of Si at the grain boundary. In addition to these, they also observed some other features in the micrographs e.g. thick boundary layers, second phase particles, triple point agglomerates and dopant precipitates. Thick boundary refers to amorphous grain boundary layers which are at least 3-50 nm thick. Second phase particles consist of Si mainly and are also amorphous. Triple point junctions serve as sinks for all other impurities in addition to Si. Gerhardt et al. proposed that grain boundaries effect can be reduced either by increasing dopant concentration or doping with large size cations. They react with silica and form some silicate phases which gather at the triple point junctions. In yttrium doped ceria, some precipitate was found containing phases of yttrium silicates e.g. $Y_2Si_2O_7$ and Y_2SiO_5. These precipitates increase in the quantity as the yttrium content increases [Gerhardt et al. (1986)].

A blocking factor, α_R, was proposed by Gerhardt et al. to evaluate the influence of grain boundaries conductivity on the total conductivity. α_R gives the fraction of charge carriers being blocked at the impermeable internal surface,

under the measuring conditions, with respect to the total number of charge carriers in the samples.

$$\propto_R = \frac{R_{gb}}{R_g + R_{gb}} \tag{1.20}$$

where, R_g and R_{gb} are resistance of the grains and grain boundaries.

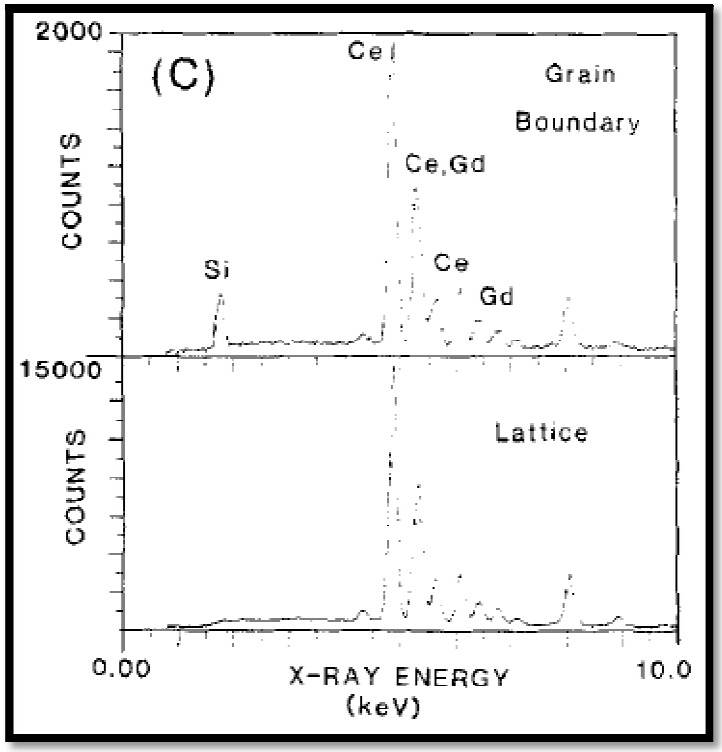

Fig. 1.8 EDXM spectra of a grain and grain boundary in CeO_2:6 mol% Gd_2O_3 sample. Unlabeled peaks are due to contaminants from milling [Gerhardt et al. (1986)]

1.12 Conduction Mechanism and Temperature Dependence of Ionic Conductivity, Activation Energy and Pre-Exponential Factor

The electrical conductivity, σ is given as:

$$\sigma = ne\mu \tag{1.21}$$

where, n, e and μ are the concentration of the charge carriers, electronic charge and mobility respectively. Mobility is defined as the velocity per unit field

strength. It is a measure of the swiftness of the charge carriers in the applied electric field. In the case of the oxide ion conductor, conduction occurs through oxygen ion vacancies. Equation 1.21 is, therefore, written as:

$$\sigma_v = N_v q_v \mu_v \tag{1.22}$$

The suffix 'v' represents the vacancy and N_v is the number of oxygen vacancy per unit volume. A relation between the mobility μ and the diffusivity D is given by Nernst-Einstein equation as:

$$\mu = qB = qD/kT \tag{1.23}$$

where, B is the absolute mobility i.e. the velocity v_i, obtained under the action of a unit force. Diffusivity, D, is given as:

$$D = a^2 \vartheta_0 exp\left(\frac{\Delta S_m}{k}\right) exp\left(-\frac{\Delta H_m}{kT}\right) \tag{1.24}$$

where, 'a' is the jump distance of a vacancy, ν_0 is the vibrational frequency and ΔS_m and ΔH_m are the activation entropy and the activation enthalpy of diffusion respectively. N_v is written as:

$$N_v = [V_O^{\bullet\bullet}][1 - V_O^{\bullet\bullet}]N_O \tag{1.25}$$

where N_O is the number of oxygen sites per unit volume. Using Eqs. 1.22, 1.23, 1.24 and 1.25 it follows:

$$\sigma T = A' [V_O^{\bullet\bullet}][1 - V_O^{\bullet\bullet}] exp\left(-\frac{H_m}{kT}\right) \tag{1.26}$$

$$A' = (4e^2/k) a^2 \vartheta_0 N_0 \, exp\left(\frac{\Delta S_m}{kT}\right) \tag{1.27}$$

For small value of $V_O^{\bullet\bullet}$ Eq. 1.26 is written as:

$$\sigma T = A' [V_O^{\bullet\bullet}] exp\left(-\frac{H_m}{kT}\right) \tag{1.28}$$

It is concluded from the above relations that the temperature dependence of the electrical conductivity cannot be expressed by a single exponential term. The plot of conductivity vs. temperature has three regions, I, II and III. Region I appear in the high temperature range in which the electrical conductivity is determined by the intrinsic defects i.e. Schottky or Frenkel defect in the lattice. In region II, conductivity is controlled by the concentration of charge carrying defects caused by aliovalent dopants or the impurity presents at the boundaries (discussed in detail in section 1.11). Region III appears in the low temperature range. In this

region, concentration of charge carrying defects is determined by the thermodynamic equilibrium between the free defects and associated defect pairs. Ceria oxide doped with aliovalent cations has large number of oxygen vacancies, therefore, it only has the regions II and III.

Kilner et al. (2000) suggested that the association energy is a function of columbic attraction between the oxygen vacancies and dopants and the elastic strain present in the lattice. The type of associate pairs formed depends on the charge of the dopant used. For e.g., a neutral associate defect pair $[M''_{Ce} - V_O^{\bullet\bullet}]^{\times}$ will form whereas charged pair $[M'_{Ce} - V_O^{\bullet\bullet}]^{\bullet}$ will form when divalent and trivalent cations are used respectively.

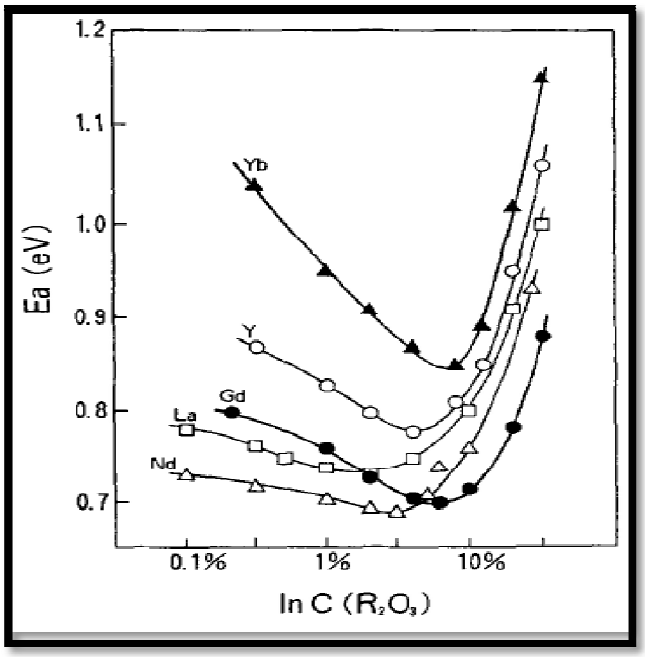

Fig. 1.9 Variation of association energy against the dopant concentration for various rare earth cation doped ceria [Fabor et al. (1989)]

Due to charged nature of the pair for trivalent dopants, binding energy of this pair depends on the concentration of the dopant due to columbic attraction and shows a minimum [Kilner (1982)]. The relation between the electrical conductivity, activation energy and temperature is given by Arrhenius equation as given below:

$$\sigma T = \sigma_0 \exp\left(\frac{-E_a}{KT}\right) \tag{1.29}$$

where σ_0 is a pre-exponential factor, T is the absolute temperature and E_a, is the activation energy of conduction. At low temperatures, activation energy for conduction in doped ceria is given by the sum of association energy (E_A) and the migration energy (E_m) [Inaba et al. (1996)]. Association energy results from electrostatic attraction between the dopant cations and the oxygen vacancies $[M''_{Ce} - V_O^{\bullet\bullet}]$. This decreases the number of free oxygen vacancies available for conduction.

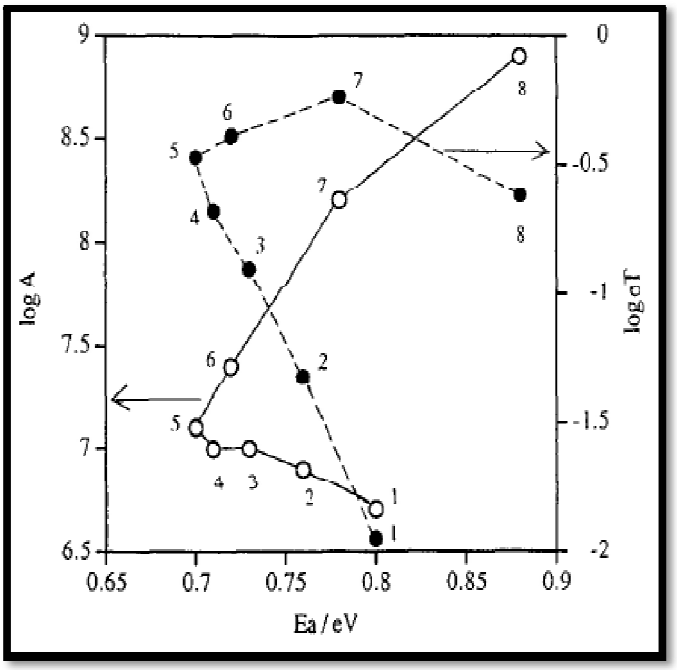

Fig. 1.10 Log σT and Log A vs Ea (activation energy) plot of yttria-doped ceria [Fabor et. (1989)] (1) 0.05 mol% (2) 0.15 mol% (3) 0.5 mol% (4) 1 mol% (5) 2 mol% (6) 4 mol% (7) 6 mol% (8) 10 mol% and (9) 15 mol%

E_A also depends on the effective charge, size of the dopant and the cation polarizability [Inba et al. (1996)]. As temperature increases, the associated defect pairs dissociate and oxygen vacancies become free. At higher temperatures, therefore, migration enthalpy of oxygen ion is the total activation energy of conduction. Fabor et al. (1989) studied the variation of association energy with the dopant concentration. Fig. 1.9 shows the variation of association energy with the dopant concentration. It shows a minimum value at a certain concentration and increases thereafter.

Shannon et al. (1969) proposed the critical ionic radius in order to obtain minimum strain in the lattice. The critical ionic radius for divalent and trivalent cations was calculated as 1.106 and 1.038 Á respectively. They also determined the deviation of lattice parameter from the hypothetical pure zirconia in the system of ZrO_2-ThO_2-Y_2O_3 and found that the activation energy of conduction can be correlated with the deviation of lattice parameter [Kim (1989)].

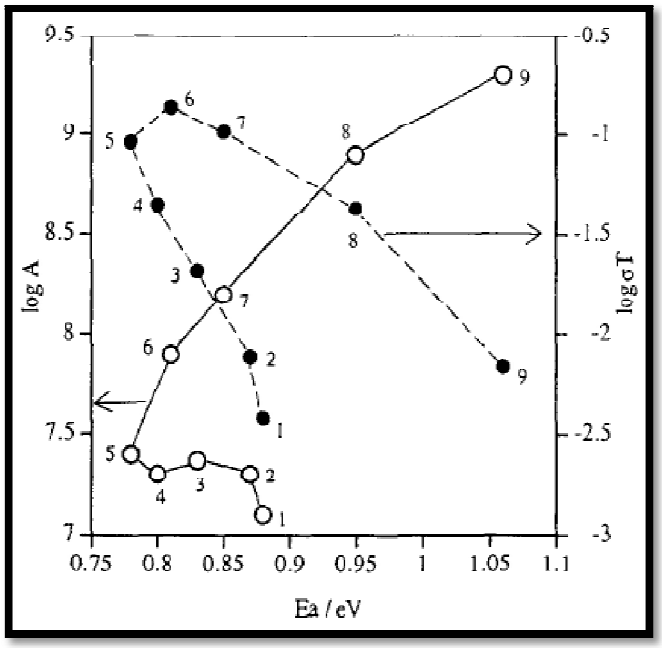

Fig. 1.11 Log σT and Log A vs Ea (activation energy) plot of gadolinia-doped ceria [Fabor et. (1989)] (1) 0.1 mol% (2) 0.5 mol% (3) 1 mol% (4) 2 mol% (5) 3 mol% (6) 5 mol% (7) 10 mol% and (8) 15 mol%.

Faber et al. (1989) studied the variation of electrical conductivity and pre-exponential factor with the activation energy of yttria and gadolinia doped ceria [Fig. 1.10 and 1.11 where the numbers denote the order of concentration]. Activation energy decreases significantly as the concentration of dopant increases while the pre-exponential factor remains constant. The maximum electrical conductivity is obtained at a higher concentration than that of minimum activation energy. It is also observed from these two plots that the maximum of electrical conductivity and the minimum of activation energy are not always associated with the same dopant concentration because pre-exponential factor is also a function of the dopant concentration. From Figs. 1.10 and 1.11 it is noted that the

concentration which gives the maximum conductivity is quite different between yttria and gadolinia doped ceria as shown in Figs. 1.10 & 1.11. Pre-exponential factor starts to decrease at higher concentrations. It may be due to partial ordering of the defects.

1.13 Dual Phase Ceria Based Composites

The single phase ceria based solid electrolytes have been studied and extensively used for IT-SOFCs. Some disputes, however, reduces their commercialization and applications. Doped ceria electrolytes possess some electronic conduction in a reducing environment due to conversion of Ce^{4+} to Ce^{3+} [Doshi et al. (1999); Godickemeier et al. (1996); Li et al. (1998)]. This results in internal short circuiting and decreases the open circuit voltage and reduces mechanical strength also. Dual phase ceria/salt based composites have been widely studied to remove all these problems [Zhu et al. (2006)]. Many ceria based composites have been investigated such as; ceria/hydrate, ceria/perovskite oxide and ceria/salt based composites for next generation fuel cells.

1.13.1 Ceria-hydrate composites

In ceria/hydrate dual phase composites, one phase is ceria and the other phase is hydrate such as NaOH, KOH [Zhu et al. (2006)]. Ceria-hydrate composites have conduction from both the ions (O^{2-} and H^{+} ions). Oxide ions conduction takes place through ceria phase and H^{+} conduction occurs from hydrate phase as well as via the interfaces formed between the ceria and hydrate phases. Conduction of OH^{-} ions also occurs when the temperature increases above the melting point of the hydrates. Due to dual ion conduction in ceria/hydrate composites, a power density of 800mW/cm^2 was found at 600 ºC [Liu X.R. et al., 2004]. The drawback of using this composite is that the hydrates react with CO_2 and forms carbonate. This creates problem for alkaline fuel cell (AFC) where the conducting ion is the OH^{-}.

1.13.2 Ceria-perovskite oxide composites

Perovskite oxides of general formula ABO_3 have sufficient proton conductivity at higher temperature on exposing to a humid atmosphere [Jie et al. (2006)].

Recently, $BaCeO_3$ based perovskite oxide have attracted great interest. Further, enhancement in the ionic conductivity was observed by doping with rare earth cations such as; Y^{3+} and Gd^{3+}. Perovskite based oxide can, therefore, be used as a second phase in doped ceria electrolyte to form the dual phase composite. IT-SOFC based on $Ce_{0.80}Gd_{0.20}O_{1.90}/BaCe_{0.90}Y_{0.10}O_{3-\delta}$ (SDC/BCY) composite has a power density of >300 W/cm^2 at 550 ºC [Zhu et al. (2004)]. Schober et al. [Schober et al. (2004)] reported that a superionc transition occur around 550 ºC in the conductivity plot. This is attributed to the interfacial superionic conduction at the interfaces formed between ceria and the perovskite phases. Conductivity of the composite is much higher than the conductivity of each individual phase.

1.13.3 Ceria-salt based composites

Similar to pervoskite based oxides, salts also have proton conduction and in the composite electrolyte, it conducts through the interfaces of two phases [Zhu (2006); Zhu et al. (1994); Zhu (1996); Zhu (2001)]. Salts, however, cannot be used in SOFCs due to high working temperature. Among various ceria/salt composites $SDC/(Li\text{-}Na)_2CO_3$ (SDC/LNCO) shows a maximum conductivity of 10^{-1} S/cm in the low temperature region [Zhu et al. (2006)]. SDC/LNCO composite contains one molten phase at working temperature of the fuel cell. Molten carbonates fill the interspaces between the SDC particles and create a large interfacial region between the two phases. Due to interfacial effects, a small amount of the molten carbonate phase enhances the ionic conductivity significantly. But, this not weakens the mechanical strength. The electrolyte remains as a solid phase [Zhu et al. (2006)]. In addition to O^{2-}, CO_3^{2-} ions also contribute to the conductivity when the temperature increases above the melting point of the carbonates. Multiions conduction, therefore, improves the performance of the SOFCs.

1.14. Nanocomposite Idea

An idea of nanocomposite was given by Zhu et al. [Zhu et al. (1999); Zhu (2001); Zhu et al. (2003); Fu (2002); Zhu et al. (2002); Liu et al. (2004); Hu et al. (2006)]. Nanocomposite is the mixture of nanosized ceria powder and the carbonates. Fine particles having high surface energy will produce large interface region available for the interaction between the two phases.

Interaction does not mean the chemical reaction since no new phase and ions diffusion take place between two phases [Fan et al. (2013)]. Smaller the particle size of the ceria phase, larger will be the interfacial region which leads to superionic conduction at very low temperatures (300-600 ºC). This results in a new class of SOFCs i.e. low temperature solid oxide fuel cells (LT-SOFCs). In addition, large interfacial region will increase the density of mobile defect in the space charge region [Arico et al. (2005)]. It can be concluded, therefore, that particle size of the composites prescribes the total conductivity. Among different composite electrolytes, doped ceria/carbonate composite is the most promising electrolyte for LT-SOFCs [Zhu (2001); Wang et al. (2008); Chen et al. (2010); Fan et al. (2011); Wang et al. (2011)]. In ceria/ carbonate composites carbonates exist as an amorphous phase and covering the ceria particle.

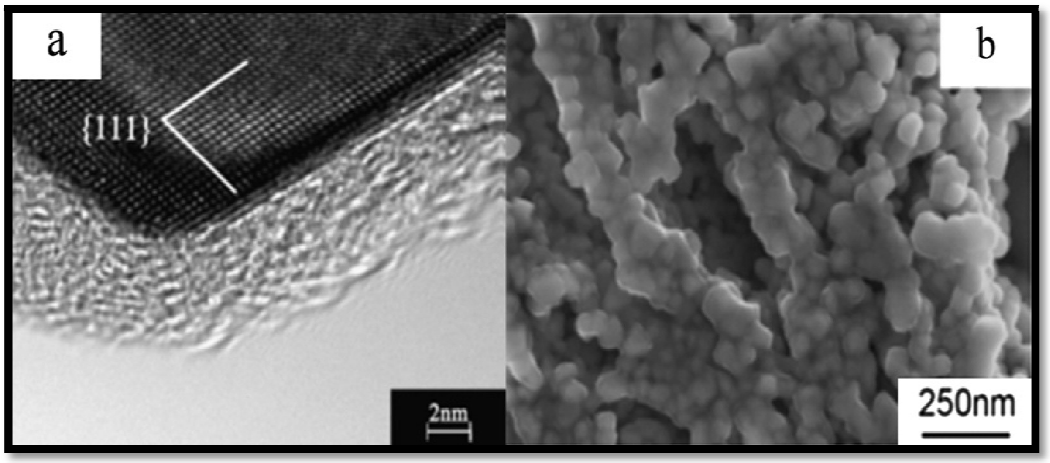

Fig. 1.12 (a) TEM images and (b) SEM images of ceria/carbonate nanocomposite [Wang et al. (2008); Lapa et al. (2010)]

An early stage of sintering of the composites gives a good densification because carbonates melt at the working temperature and fills in the interspaces uniformly. Wang et al. (2008) and Lapa et al. (2010) studied the morphology of doped ceria/carbonate composite electrolyte using high resolution transmission electron microscope (HR-TEM) and scanning electron microscope (SEM) [Fig. 1.12a and 1.12b]. TEM image shows a core-shell type structure in which ceria is the core and carbonate is the shell. Carbonates show amorphous structure while ceria is

present as a crystalline phase at room temperature. It can also be noticed that interface phase is different from both the crystalline and amorphous phase. This interface builds high speed ionic pathways for conduction. SEM image indicates that the nanosized ceria particles are surrounded by the carbonate phase. Gao et al. (2011) studied the performance of SDC/Na_2CO_3 based fuel cells. They reported that SDC/Na_2CO_3 nanocomposite shows conductivity several times higher than that of the SDC/Na_2CO_3 microcomposite. Nanocomposite shows more complex grain boundary interfacial effects than that of the microcomposites. Nanocomposites have higher AC conductivity and low activation energy especially at low temperatures [Gao et al. (2011)].

1.15 Effect of Carbonate Composition and Concentration

Electrochemical performance of ceria/carbonates composite based low temperature fuel cells shows the divergences from different carbonate compositions and contents.

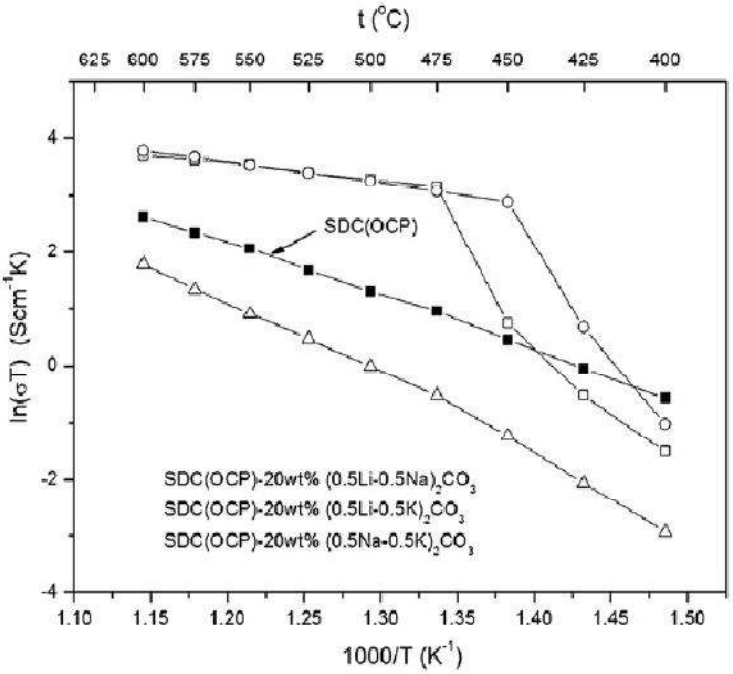

Fig. 1.13 Variation of ionic conductivity of the composites electrolyte with carbonate compositions [Zhao et al. (2012)]

Its highly depends on the microstructure and other parameters such as particle size, morphology, gas atmosphere etc. not only on the composition. It was also

previously reported by other researchers that low temperature fuel cells based on ceria/carbonate composites show high power density than that of fuel cell based on single phase doped ceria electrolytes or MCFC with Al_2O_3-carbonate composite electrolyte [Zhang et al. (2009); Song et al. (2011)].

Effect of carbonate composition on the electrical performance was studied by Huang et al. (2010). Results are shown in Fig. 1.13. It is noted that a sharp conductivity leap appeared for composite electrolyte with Li_2CO_3 and others carbonate at 475 and 450 ºC respectively.

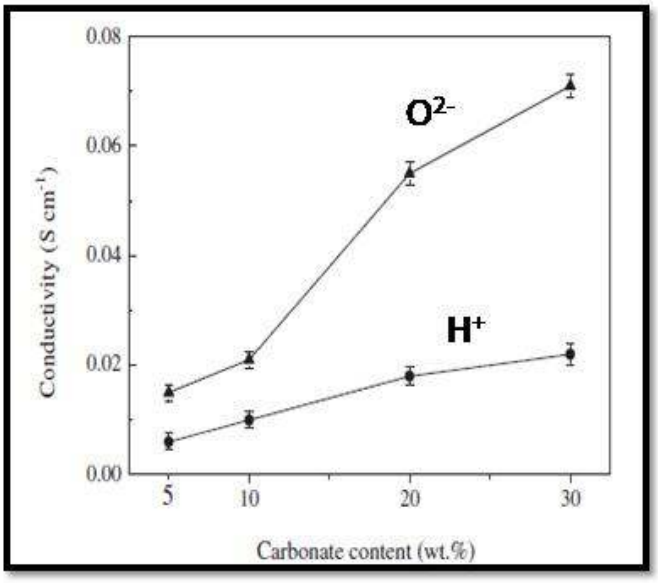

1.14 Variation of conductivity with carbonate content at 650 °C [Zhao et al. (2012)]

Conductivity of SDC/(Na-K)$_2CO_3$, however, increased linearly with temperature and one order of magnitude lower than that of SDC. However, electrochemical performance of the fuel cells based on above composite electrolytes does not follow the same trend. Single cells based on SDC/(Li-K)$_2CO_3$ and SDC/(Na-K)$_2CO_3$ composite electrolytes show power density close to each other and higher than those of SDC based SOFCs. It was concluded therefore that for ceria carbonate composites power outputs are different for ionic conduction behaviors, charge carriers and their transport pathways respectively in air or in fuel cell conditions. Liu et al. (2010) investigated the DC oxygen ion conductivity of Sm^{3+}-

Nd^{3+}/(Li-Na)$_2CO_3$ composite electrolyte. They reported that DC conductivity is not proportional to carbonate content. The optimum ratio was 80:20 for SDC to carbonate. AC conductivity depends on the contribution of all mobile ions such as; O^{2-}, CO_3^{2-}, Li^+ and Na^+. Liu et al. (2010) also reported that superionic conduction transition temperature changed with the carbonate content.

Zhao et al. (2012) studied the O^{2-}/H^+ conduction in the SDC/($Li_{0.52}$ $Na_{0.48}$)$_2CO_3$ composite electrolyte by electrochemical pumping. They found that conductivity of both O^{2-} and H^+ ions increases with increasing carbonate content. Variation of conductivity of composites with carbonate content is shown in Fig. 1.14. Conductivity of O^{2-} is higher than that of H^+ ion. They suggested that in addition to the SDC phase, carbonate phase also conduct O^{2-} ions. In the SDC/30($Li_{0.52}$ $Na_{0.48}$)$_2CO_3$ composite, conductivities of O^{2-} and H^+ ions were found to be 0.071 S/cm and 0.022 S/cm respectively at 650 ºC. Both of these values are higher than that of the pure SDC phase suggesting that molten carbonate phase facilitates the conduction of both the ions. Enhancement in the conductivities of O^{2-} and H^+ ions is attributed to the interfacial effects in the nanocomposites [Feng et al. (2006)].

From the above interpretations, it is concluded that ceria/salt composites have mixed ionic conduction due to O^{2-}, H^+ and/or CO_3^{2-} ions. Conduction due to O^{2-} ions occurs in the ceria phase. Conduction of CO_3^{2-} ions takes place in molten carbonate above the melting point of the carbonate binary mixture [Zhao et al. (2012)]. Due to equilibrium of CO_3^{2-} and O^{2-} ions in the molten carbonate phase as given by Eq^n.1.22, a slight solubility of O^{2-} in the carbonate exists.

$$CO_3^{2-} \leftrightarrow CO_2 + O^{2-} \tag{1.30}$$

Zhao et al. (2012) also reported that in ceria/carbonate composite electrolytes, conductivity of O^{2-} ions is higher than that of H^+ ions. They suggested that O^{2-} ions are the intrinsic charge carriers in both the ceria and the molten carbonate phase while H^+ ions are extrinsic in the carbonate phase. Zhao et al. (2012) also reported that concentration of O^{2-} ions is higher than that of H^+ ions in both the phases.

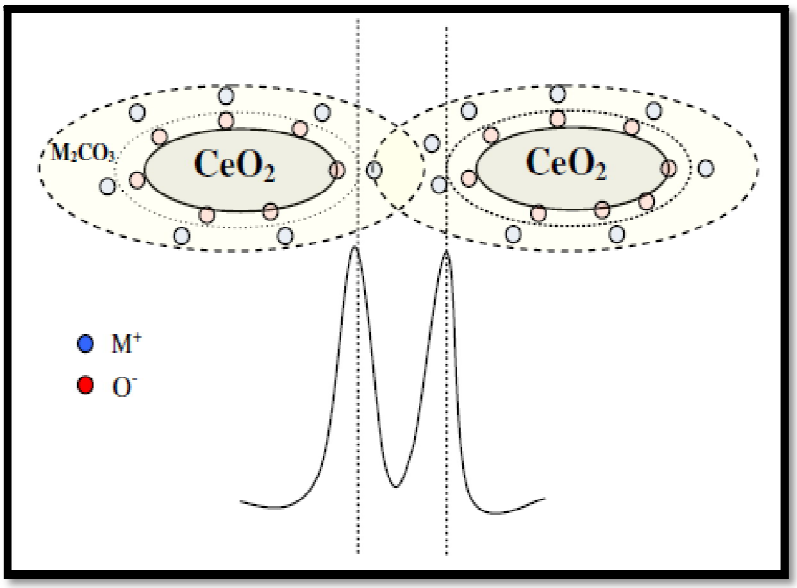

Fig. 1.15 Electrical field at the interfaces between two constituent phase particles [Zhu B. et al., 2008]

Questions are that; (i) how is the extrinsic nature of H^+ ion conduction in the ceria/salt composites? (ii) It was also given by other researchers that conduction of H^+ occurs via an intermediate HCO_3^-. Then, why does the performance of MCFC is inferior to that of ceria/salt based composite fuel cells using the similar electrolytes? (iii) How does the dual ion conduction occur in the composites? Zhu et al. [Zhu (2003); Zhu (2006); Zhu et al. (2008)] proposed an interfacial conduction mechanism to explain the enhanced oxygen ion conductivity of ceria/salt based composites. Due to presence of high concentration of O^{2-} ions/defects on the ceria particles surface and interfacial interaction between the two phases may constitute an ionic conductive highways for O^{2-} and H^+ ions in the ceria carbonate composite electrolytes. It was reported by Zhu et al. (2008) that the electric field distribution in the interfaces is a key for interfacial ionic conduction. The interactions between the oxygen ions on the ceria particle and M^+ ions (Li^+, Na^+ and K^+) of the carbonate leads to an electric field at the interfaces as shown in Figs. 1.15 and 1.16. The potential can be described as:

$$E = K\frac{1}{4\pi\epsilon_0\epsilon}\frac{Qq}{R} \tag{1.31}$$

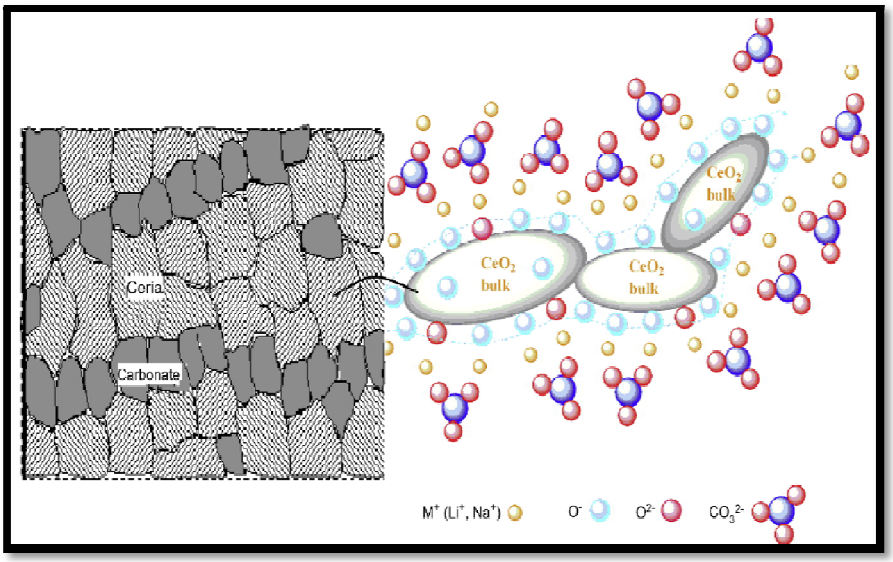

Fig. 1.16 Conducting highways at the interfaces of two phase particles resulting in interfacial superionic conduction [Zhu et al. (2008)]

where Q =2e for O^{2-} or 1e for O^{-} and q = 1e for M^{+}. K < 1 because the effective charge between O^{2-} and alkaline cation is not entirely affiliated to interaction, ε is the average dielectric parameter for ceria and carbonate and r is the distance between M^{+} and O^{2-} ions.

Wang et al. (2011) proposed a model known as 'Swing Model' to explain the mechanism of super proton conduction in SDC/Na_2CO_3 nanocomposite. According to this model, a long chain hydrogen bond (Ce-O----H----O-CO_2^{2-}) formed provides highways for proton conduction. Above a critical temperature bending-stretching vibrations of the C-O bond and mobility, rotation of the CO_3^{2-} group make the H^{+} conduction easy under the electric field. This model, however, does not explain the conduction mechanism in other composites in which O^{2-} ions play a dominant role [Chen et al. (2010)]. At present study of ionic transport mechanism in a composite electrolyte is still in progress.

1.16 Stability of SOFCs Based on Ceria/Carbonate Composite

1.16.1 Materials thermal and chemical stability

As a potential candidate for LT-SOFCs, composite electrolytes should have high chemical and thermal stability during long time of operation.

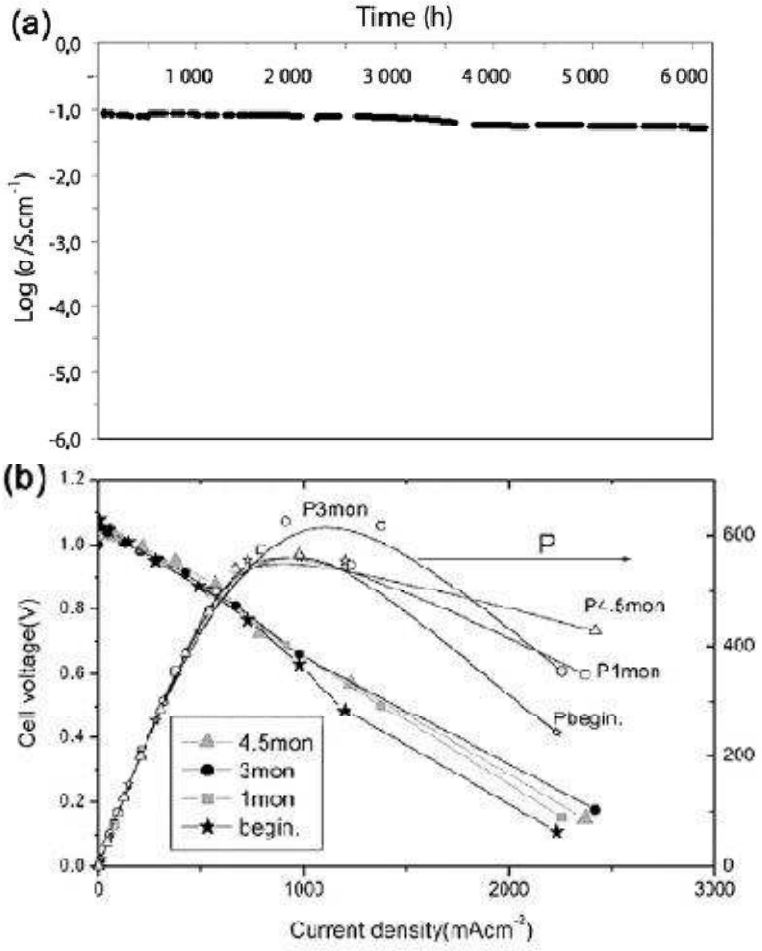

Fig. 1.17 (a) Time dependence of electrical conductivity of GDC/(Li-K)$_2$CO$_3$ composite at 600 ºC in air under OCV condition [Benamira et al. (2012)] (b) Evaluation of cell performances vs. time for ceria/carbonate composite electrolytes based SOFC at 550 ºC [Zhu et al. (2003)]

Benamira et al. (2011) have made a systematic investigation on the thermal, structural and morphological properties of GDC based composite materials. They found that there is no weight loss during thermal cycling from room temperature to 700 ºC and an aging of 168 h at 500 ºC. Ma et al. (2010) suggested that due to the typical core-shell structure of nanocomposites, no volatization or weight change occurs after thermal cycling from 400-800 ºC. The stability of nanosize particles is a major factor for high temperature operation. In ceria/carbonates nanocomposites, grain growth in the ceria phase is suppressed by carbonate phase resulting in separate nanoparticles with large surface area. This is an advantage of

nanocomposites compared to single phase SDC where agglomeration occurs after heating at 700 ºC for 2 h [Fan et al. (2013)].

1.16.2 Electrochemical stability

There are many results reported by the researchers on the electrochemical stability of ceria based nanocomposites. Li et al. (2011) have studied the stability of ceria/carbonates composite after testing for the period of 3 days and observed a constant ionic conductivity. Benamira et al. (2012) have reported the conductivity test up to 6000 h as shown in Fig. 1.17 (a). A high AC conductivity above 0.07 S/cm has been found during long term stability test.

Huang et al. (2006) also suggested the stability of SOFC using composite electrolyte up to 36 h, no degradation was observed. They also suggested that the stability can be further enhanced by using CO_2 at the cathode along with O_2 to maintain the phase and concentration of carbonate in the composite electrolyte. Zhu et al. (2003) studied the performance of SDC/20 wt% carbonate up to 4.5 months at 550 ºC with H_2 as a fuel and air as the oxidant as shown in Fig. 1.17 (b). They found an enhancement in the maximum power density up to 3 months and then a reduction after 4.5 months, indicating a good stability in fuel cell condition. The reduction in the cell performance after 3 months is due to dissolution of Ni from the cathode into the molten carbonate in the composite. Therefore the development of novel cathode is an important issue. The stability for 100 h was observed for ceramic fuel cells (CFCs) with ceria/carbonate composite electrolyte using $Sm_{0.5}Sr_{0.5}Fe_{0.8}Cu_{0.2}O_{3-\delta}$ cathode [Fan et al. (2013)].

1.17 Applications of SOFCs Technology

SOFCs technology has been developed for large scale power generation applications. It ranges from portable devices, auto mobile auxiliary power units to distributed power generation. The concept of some applications is discussed as below:

1.17.1 Stationary power generation

Tubular design SOFCs have been developed as the power generation system up to 250 kW size [Singhal (2000)]. Siemens Westinghouse fabricated an atmospheric power generating system of 100 kW size [Singhal (2000)]. In this power system SOFC stack consists of 1152 cells (2.2 cm diameter and 150 cm active length cells) which are arranged in 12 bundle rows. It was successfully operated for 2 years in the Netherlands on de-sulfurized natural gas without any substantial degradation. It provided up to 108 kW of ac electricity at an efficiency of 47% to the Dutch grid and approximately 85 kW of hot water for the local district heating system.

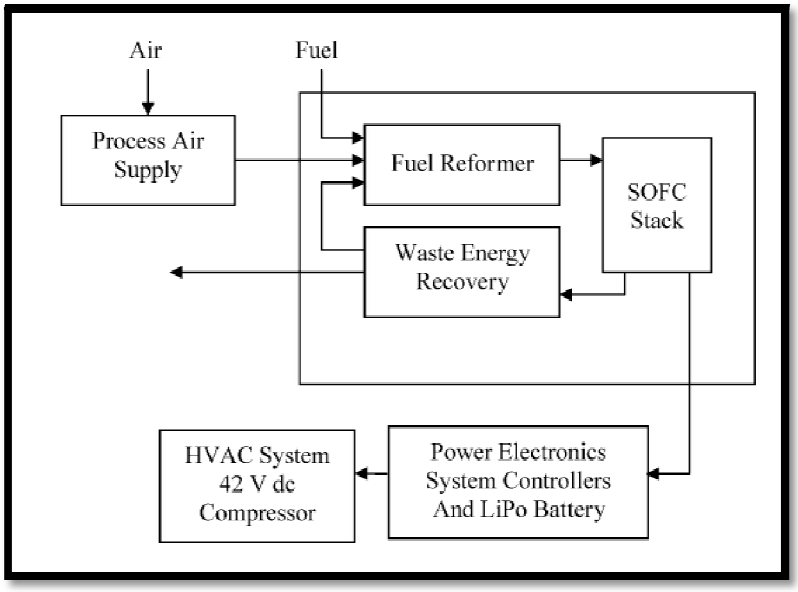

Fig. 1.18 Basic building block for automobile APUs [Singhal (2000)]

1.17.1 Transportation

The polymer electrolyte membrane fuel cells (PEMFCs) are generally used for transportation application but it possesses some disadvantages related to the overall cost [Singhal (2000)]. PEMFC uses only H_2 as a fuel with no CO to operate successfully. At present, however, no infrastructure exists to produce H_2. Furthermore, it is also difficult to remove CO from the reformate system. However, SOFCs can use variety of fuels. Due to high operating temperatures and availability of water on anode side makes reforming of hydrocarbon fuels possible. The initial application of SOFCs is in on-board auxiliary power units

(APUs). These APUs operating on existing fuels will initially supply for increasing electrical power demands for luxury automobiles, vehicles and heavy trucks. The basic building block for automobile auxiliary power units is shown in Fig. 1.18.

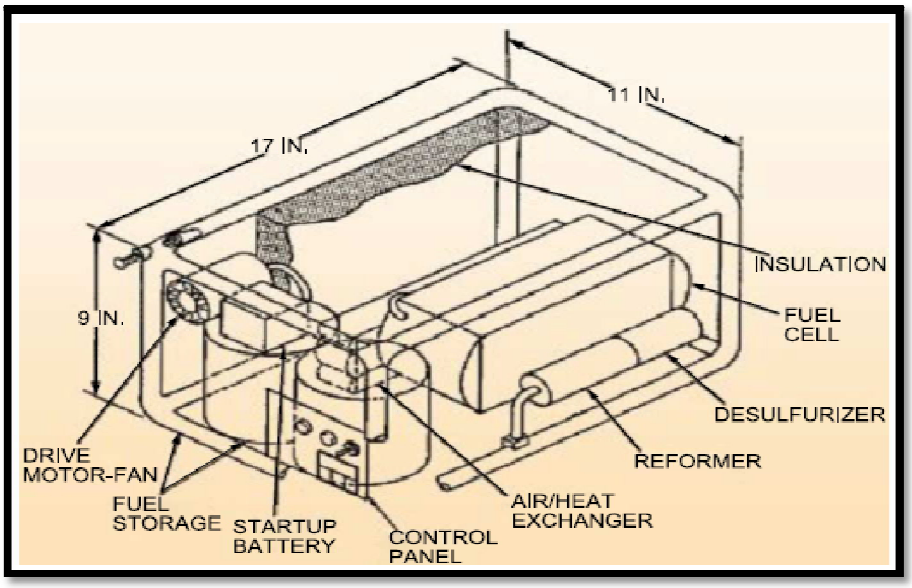

Fig. 1.19 500 W battery charging system concept [Minh (2004)]

Fig. 1.20 Portable SOFC system [Minh (2004)]

1.17.3 In military sector

Planer SOFCs having high power density ~2 W/cm^2 are well suited for military applications. These include ship service power and ship propulsion, air force bare base tent city power, army ground vehicles, mobile power generators and soldier power. A 5 kW automotive APU using anode supported planer SOFC is being developed by Delphi Automotive Systems to power an AC electric system without the need of operating vehicle engine [Zizelman et al. (2000)]. Fig. 1.19 shows a 500 W portable SOFC power system operating on jet fuels (JP-8) for military applications [Minh (2004)]. The system produces 28 V and has approximate weight of 7 kg in a volume of 17×11×9 inch. A portable SOFC based on this concept is shown in Fig. 1.20.

1.18 Advanced Applications of SOFC Based on Dual Phase Ceria Based Electrolytes

Due to high ionic conductivity at low temperature and excellent electrochemical performance ceria/carbonate based nanocomposites have so many applications. Similar to conventional SOFCs, nanocomposites can also be used in electrolysis mode [Zhu et al. (2006)]. Multi-ion conduction of ceria/carbonate based composites intimates the different applications as shown in Fig. 1.21.

1.18.1 Solid oxide electrolysis cell

Solid oxide electrolysis cell (SOEC) is a reverse process of SOFC. SOFC based on ceria/carbonate composites can produce H_2 and O_2 from water by inputting the electricity as energy. Zhu et al. (2006) had proved the feasibility of doped ceria nanocomposite electrolyte in the electrolysis. Working principle of SOEC is based on Faraday's law.

1.18.2 Direct carbon fuel cell (DCFC)

DCFC is very famous due to its high theoretical efficiency and copiousness of solid state energy sources like wood, biomass. These are easily converted to carbon or directly oxidized to obtain electricity without the combustion.

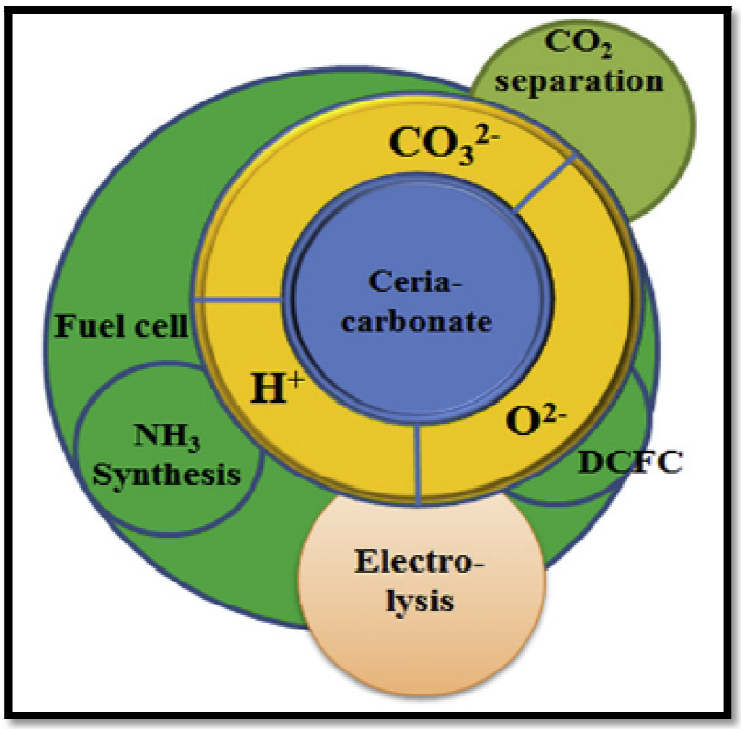

Fig. 1.21 Multi-ion conduction and advanced applications of ceria/carbonate nanocomposites [Fan et al. (2013)]

In the case of conventional single phase ceria based electrolytes, due to limited contact/interface between the carbon and electrolyte causes large electrode polarization resistance. Ceria/salt based composite electrolytes could ease this problem to some extent. At an elevated temperature, the molten salt provides more contact area and improves the cell performance [Jia et al. (2010)]. A high performance of 100 mW/cm^2 can be achieved at 700 ºC with mixed CO_2/O_2 cathode gas, making the DCFC an assuring energy device [Jia et al. (2010)].

1.18.5 Synthesis of ammonia

Proton conduction in the ceria/carbonate composite had been employed for electrochemical synthesis of ammonia. A fuel cell using SDC/$(Li\text{-}Na)_2CO_3$ composite electrolyte with H_2 gas in the anode chamber and N_2 in the cathode chamber produces ammonia at the rate of 5.39×10^{-9} mol $s^{-1}cm^{-2}$ at 450 ºC [Zhu et al. (2004)].

1.18.6 CO_2 separation

Capturing of CO_2 and its storage is a worldwide anxious topic since the innovation of green house gas effect [Fan et al. (2013)]. For this purpose CO_2 should be separated from the other gases. Dual ion conduction in ceria/carbonate composite electrolytes makes it possible to separate CO_2 and O_2 simultaneously. It was also reported by Xia et al. (2010) that in ceria/carbonate composite electrolytes, CO_3^{2-} ion conduction takes place via molten carbonate and O^{2-} conduct through bulk ceria phase. Dual ion conduction does not need the external oxygen associated transport anymore. CO_2 separation efficiency of GDC/carbonates composite electrolyte was studied by Wade et al. (2011, 2008). They found that the flux of CO_2 across these membranes has reached permeability of 10^{-11} mol/m-s-pa at 850 ºC. Except these advanced applications, ceria/carbonate based nanocomposites hold vision for other fields such as chemicals and electricity co-produce, solid sulfur recycle and consumption [Liu et al. 2004].